Part 1

Guidelines for Book Preparation in MS Word using WSPC Style

Chapter 1

Peptide-based methods for the assembly of plasmonic nanostructures

1.1 Introduction

Nanostructures are a family of materials that have at least one dimension between 1 and 100 nm [1]. Compared to bulk materials, nanostructures are particularly exciting because they exhibit unique and sometimes exceptional size-dependent chemical [2], physical [3], and/or biological [4-6] properties. Control over the size, shape, and composition of nanostructures allows for fine-tuning their fundamental properties [7]. Furthermore, ensembles of nanostructures gives rise to the emergence of new collective properties, especially when they are precisely organized with respect to one another in a hierarchical manner. In summary, nanostructures and their assemblies are immensely promising materials having exciting complex functional capabilities [8-11].

Inorganic nanostructures, in particular have attracted intense attention over the last two decades. For example, research on metallic nanoparticles, semiconducting nanoparticles [12], and metal oxide nanoparticles is expanding constantly due to their potential in bio-imaging [11, 13, 14], drug delivery [15-19], bio-sensing [5, 14, 20-22], and catalysis [2, 23-26]. Their performance and properties can be tuned and optimized by rational design and systematic tuning of their composition, size, and assembly architecture.

To construct a specific nanostructured material, two common strategies are used: the "top-down" approach or the "bottom-up" approach (Fig. 1.1). The first approach usually starts from a bulk material and one or more dimensions of the material are gradually reduced to the nanometer scale. This process is analogous to how a sculpture is carved from bulk marble. While this process enables precise control over the size and shape of the resulting product, control over the hierarchy or complexity of the material, such as composition mixing or layer-by-layer arrangement, is more challenging. On the contrary, the "bottom-up" approach involves assembly of atomic, molecular, and nanoscale building blocks. This approach is simple and flexible, and the chemical and physical properties of the final nanostructure can be easily tailored by rational design and synthesis of the constituent building blocks.

The "bottom-up" approach is essentially based on the self-assembly of building blocks. Many complex systems are constructed via self-assembly. Living organisms are composed of ordered organization of cells; cells are composed of ordered organization of DNA, proteins, and many functional compartments; and even proteins are ordered organization of 20 naturally existing amino acids. These complex systems – living organisms, cells, DNA, and proteins – are functional structures assembled from only a few fundamental building blocks. Inspired by these biological precedents, materials chemists carefully fabricate building blocks and devise methods for assembling them into complex architectures.

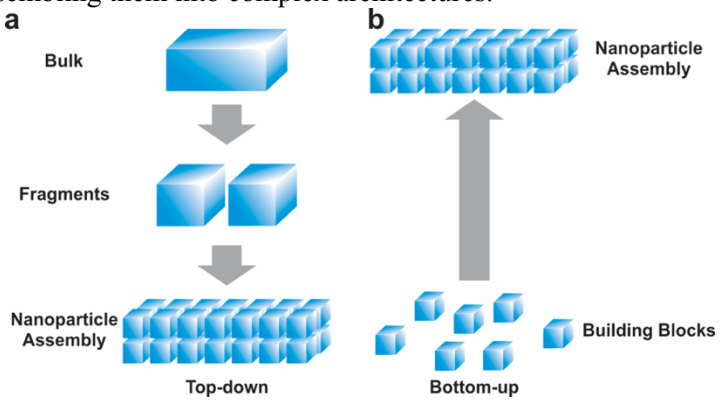

Fig. 1.1. Two strategies of constructing nanostructured materials: (a) "top-down" approach and (b) "Bottom-up" approach.

Plasmonic nanostructured materials, in particular, have been and will continue to be centerpiece materials in nanoscience research because they exhibit unique optical properties. Reducing the dimensions of certain materials to the nanoscale leads to geometric confinement of conducting electrons. When the collective oscillation of surface electrons matches the frequency of the incident light, a phenomenon called localized surface plasmon resonance (LSPR) occurs [22, 27]. Based on the composition, size, shape, dielectric environment, and/or assembly/aggregation state of the nanoparticles (NPs) [28, 29], the position of the LSPR can vary from the visible to near infrared (NIR) region of the spectrum, which allows for a wide variety of applications, especially in optical sensing [14].

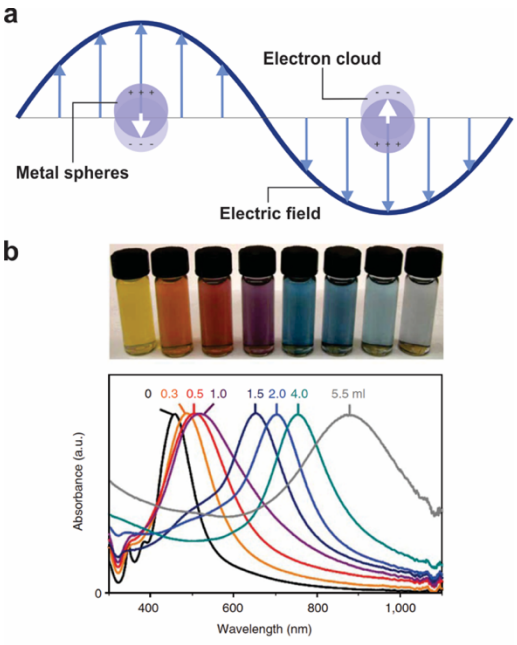

Fig. 1.2. (a) Schematic representation of localized surface plasmon resonance (LSPR) of nanoparticle. (b) Au NPs of different sizes exhibit different LSPR effect. Reproduced with permission from ref. [30]. Copyright 2007, Nature Publishing Group.

Many biomolecules, such as nucleic acids, carbohydrates, proteins [31], and peptides [32], have been used to direct the assembly of inorganic nanostructures. Biomolecules are useful in this regard, because their size is commensurate with nanoparticle building blocks and because their assembly can be controlled by carefully programming their sequence. In this chapter, we showcase the use of peptides for directing nanoparticle assembly and building complex plasmonic nanostructures with unusual and often useful collective optical properties. Peptides are sequences of amino acids, and their assembly behavior and functionality is highly sequence-specific; as a result, researchers can program and optimize the properties and performance of the nanostructure by tailoring the amino acid sequence [33]. We will highlight aspects of peptides that make them ideal for assembling nanoparticles, including their inherent ability to self-assemble and their sequence-specific inorganic recognition capability. We will examine how the field of peptide-directed nanoparticle assembly has evolved and developed over the course of the last several decades. We emphasize that this chapter is not intended to be an exhaustive review of all examples of peptide-based nanoparticle assembly. As such, we had to pick and choose examples that we feel best showcase the unique capabilities of peptides and peptide-based constructs for nanoparticle assembly.

1.2 Why Peptides?

Peptides are a family of linear biomolecules composed of amino acids. There are 20 naturally occurring amino acids and numerous non-natural amino acids that can be incorporated into a peptide. Many properties of peptides, such as their self-assembly and surface recognition properties, are sequence-specific. Tuning the sequence of amino acid residues within a peptide can lead to precise control of the overall properties of the peptide, which includes control of self-assembly architecture and inorganic surface binding.

1.2.1 *Self-Assembly of Peptides*

Peptides, along with proteins, have multiple levels of structure, with the simplest being the primary structure – the sequence of amino acids in a peptide chain. The next level of structure is the secondary structure, which is due to interactions between atoms along peptide backbone. Depending on the sequence, conformation, and stereo-configuration of the constituent amino acids, peptides can exhibit many different secondary structures, such as α-helices and β-sheets. In the context nanoparticle assembly, inter-peptide β-sheets have played an important role, especially for directing the assembly of extended linear nanoparticle assemblies (*vide infra*), because they play a key role in directing peptide fibrilization (e.g. in Alzheimer's disease [34, 35]).

Intra- or inter-peptide hydrogen bonding is the driving force for forming secondary structure. However, forming a target structure may still be challenging based solely on interactions between amino acid residues. To address this challenge, various molecules can be attached to peptides to further adjust and affect their self-assembly, thus expanding the palette of possible structures. The resulting peptide-based molecules are often called "peptide conjugates". They can assemble into various well-defined nanoscale structures such as spherical or tubular micelles or vesicles [36, 37], twisted or coiled nanoribbons [38, 39], and two dimensional nanosheets [40, 41]. Non-covalent interactions, such as hydrophobic/hydrophilic interactions, electrostatic interactions, hydrogen bonding, and π-π stacking, help drive the assembly. Not only do the conjugated moieties facilitate the formation of superstructures, but they can also introduce new functionalities, such as cell recognition [42], stimuli responsiveness [43], fluorescence labeling [44], and surface enhanced Raman resonance (SERS) applications [45], to the self-assembled structures. The conjugation of peptides with other molecules greatly expands the capabilities of peptides both as building blocks for self-assembled nanostructures and as biocompatible functional materials [46-48].

1.2.2 *Inorganic Recognition Capability of Peptides*

In addition to their self-assembly properties, peptides are also widely used for their sequence-specific recognition abilities of both biological [48-50] and non-biological materials [51]. For example, a short peptide sequence, Arg-Gly-Asp (RGD), was identified as the minimal recognition sequence within proteins in the extracellular matrix (ECM) required for cell attachment [52-54]. The RGD sequence, or sometimes a longer sequence, Arg-Gly-Asp-Ser (RGDS), has been incorporated into a variety of synthetic materials to promote cell interaction and adhesion [55, 56]. Here we focus on the role and capability of peptides to recognize, bind, promote, and direct the formation, growth, and assembly of inorganic, specifically plasmonic, nanomaterials.

Although peptides and proteins both exist in natural systems and can promote the formation of highly functional inorganic materials [57, 58], peptides are obviously less complex than proteins in terms of sequence, synthesis, and purification, and properly designed peptides could possess the same recognition sequence for inorganic materials as proteins. Indeed, many peptides (Table 1.1) that bind specifically to particular inorganic surface have been selected, identified, and isolated both in natural systems and through non-natural laboratory panning and selection methods.

Table 1.1. Examples of peptide sequences that are known to bind to plasmonic nanoparticles.

Nanoparticles	Sequence	References
Au	AYSSGAPPMPPF	[59, 60]
	DYKDDDDKP	[60]
	AHHAHHAAD	[61, 62]
	WAGAKRLVLRRE	[63]
	WALRRSIRRQSY	[63]
	MHGKTQATSGTIQS	[64, 65]
Ag	AYSSGAPPMPPF	[59]
	NPSSLRRYLPSD	[59, 66]
	SLTATQPPRTPPV	[59]
Cu	HGGGHGHGGGHG	[67]

A good example of selection from a natural system is a sequence AHHAHHAAD (HRE) from the histidine-rich protein II of *Plasmodium*

falciparum (a unicellular protozoan parasite of humans) [62], which has been found to mediate the aqueous assembly of Ag and Au clusters, in addition to several other metal sulfide and metal oxide [68] materials. Matsui and coworkers showed that the Au precursor-HRE complex forms initially, followed by nanocrystals nucleation [61].

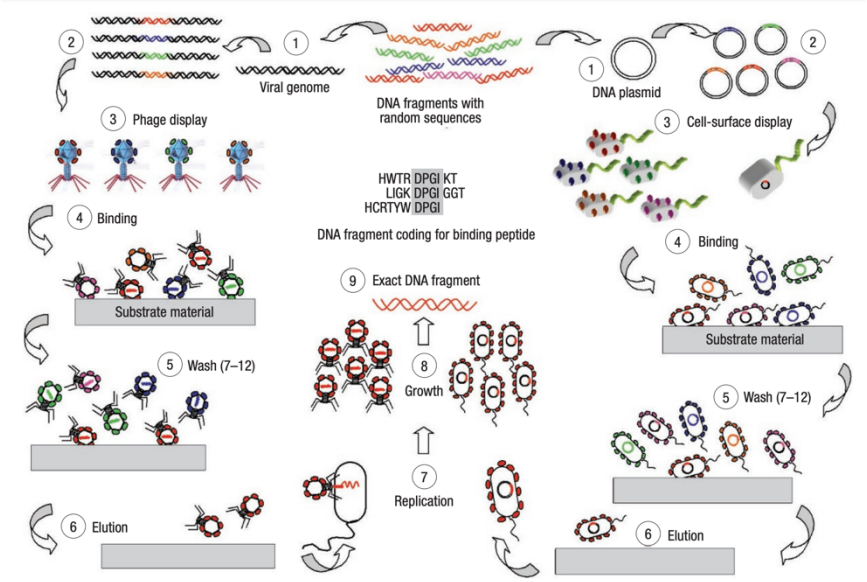

Fig. 1.3. Phage display and cell-surface display. Reproduced with permission from ref. [69]. Copyright 2003, Nature Publishing Group.

In addition to peptide sequences found in natural systems, a wider variety of peptide sequences with inorganic surface binding capabilities have been identified and selected by the phage-display method [69], which is illustrated in Fig. 1.3. This bio-panning strategy is used to isolate peptide sequences that bind strongly to the inorganic surface of interest. Apparently, the possible peptide sequences selected via phage display are only limited to the number of inorganic surfaces that are tested, thus leading to discovery of peptides having high affinity not only to plasmonic nanoparticles, such as Ag [59] and Au [70-72], but to other inorganic materials including ZnO [73, 74], GaAs [12], Pt [68, 75], Pd [68], CdS [76-78], ZnS [78], FePt [79], and Ti [80, 81]. It should be noted that many

of the peptides listed above are able to direct the mineralization of inorganic materials at room temperature and in aqueous conditions.

1.3 Peptide Scaffolds for Nanoparticle Superstructures

As discussed above, peptides are ideal candidates for constructing nanoparticle superstructures due to their unique self-assembly and surface-recognition capabilities. The process of constructing nanostructures using peptide-based materials usually involves the following steps: 1) peptides assemble into a defined template structure such as one-dimensional linear fibers or spherical vesicles; 2) synthesis and purification of constituent plasmonic nanoparticles (NPs); and 3) assembly of NPs onto constructed peptide scaffolds. Alternatively, the assembly of the peptide scaffold and the nucleation and growth of the NPs can be combined in a one-pot synthesis to yield a NP superstructure. We will present each of these methods in the following sections.

1.3.1 *Stepwise Assembly of NP Superstructures*

One of the earliest examples of peptide-directed assembly of one-dimensional AuNP superstructures was reported by Matsui and co-workers in 2002 [61] (Fig. 1.4). They showed that a histidine-rich peptide with the sequence AHHAHHAAD could be immobilized at the amide binding sites of 1-D fibers assembled using a heptane dicarboxylate molecule derivative. After incubating with a gold precursor, $ClAuMe_3$, nucleation of Au nanocrystals occurred on the surface of the fiber upon addition of a reducing agent $NaBH_4$, leading to formation of Au NP-coated nanowires. Although the peptide itself was not integral to the structure of the 1-D fiber, this unique result showcased the capability of peptides as agents for directing NP assembly onto 1-D scaffolds.

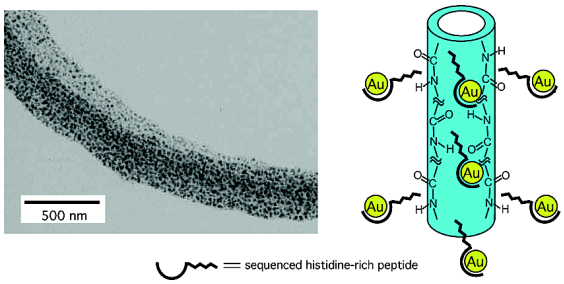

Fig. 1.4. Au nanowire templated by histidine-rich peptide nanotubules. Reproduced with permission from ref. [61]. Copyright 2002, American Chemical Society.

A short time later, in 2003, Fu *et al.* reported the preparation of double-helical arrays and single-chain arrays of Au and Pd nanoparticles based on peptide fibrilization [82] (Fig. 1.5). Peptide fibrils assembled using a synthetic 12-mer peptide, T1, served as a template for depositing pre-synthesized Au or Pd nanoparticles. The NPs anchored onto the peptide fibrils through electrostatic interactions between the positively charged peptide scaffold and the negatively charged Au or Pd NPs. It was found that the structure of the assemblies could be influenced by the pH of the reaction media and the size of the Au or Pd NPs.

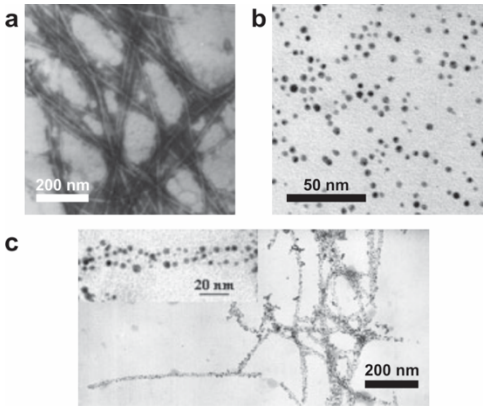

Fig. 1.5. Double-helical Au NP assembly based on peptides. TEM images of (a) T1 peptide fibrils, (b) colloidal Au NPs, and (c) double-helical assembly of Au NPs directed by T1 peptide at pH = 6. Reproduced with permission from ref. [82]. Copyright 2003, Wiley-VCH.

In addition to linear one-dimensional structures, Wong, Cha, and coworkers reported a hollow spherical assembly of silica and Au NPs using block copolypeptides [83]. The nanospheres consisted of a hollow interior, an inner layer of Au NPs, and an outer layer of silica NPs. The overall structure was mediated by a large peptide $Lys_{200}Cys_{30}$, in which the cystine section was found to be responsible for Au NP binding. Incorporation of silica enabled the assembled superstructure to exhibit exceptional robustness, hinting at possible application of the material as encapsulation agents.

Peptides could also be used to assemble Au NPs of different sizes [84]. It was reported by Langer's group that co-assembly of Au NPs of 8.5 nm and 53 nm was directed by two artificial leucine zipper-like peptides. Each peptide was engineered with a cysteine residue, which allowed the peptides to bind to Au NPs via a gold-thiolate bond (Fig. 1.6 a). By mixing the pre-synthesized NPs with the peptides, a corona-like assembly was observed, with the larger 53-nm Au NP residing in the center which were decorated with several smaller 8.5-nm NPs (Fig. 1.6 b). The assembly could be further tuned by adjusting the pH and the temperature of the solvent.

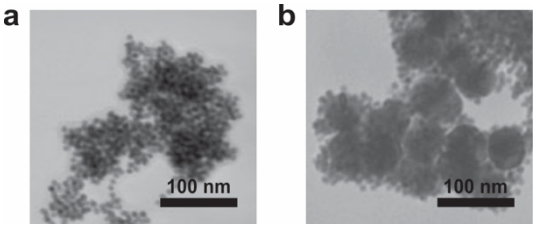

Fig. 1.6. (a) TEM image of Au NPs of 8.5 nm capped with cysteine-engineered peptide. (b) TEM images of corona-like superstructures co-assembled by two different sized Au NPs of 8.5 nm and 53 nm. Reproduced with permission from ref. [84]. Copyright 2004, Wiley-VCH.

Stupp *et al.* described the preparation of a new 1-D assembly of Au NPs via co-assembly of a tripeptide fiber-forming amphiphilic molecule and a thymine containing molecule [37] (Fig. 1.7). The co-assembly of the two molecules in organic solvent afforded nanofibers, which were then

decorated by diaminopyridine (DAP) functionalized Au NPs to yield long linear chain-like superstructures of assembled Au NPs. Diphenylalanine (FF) peptide is a popular dipeptide sequence that exhibits strong capability to assemble into nanofibers [34], and it has been employed in many cases as a nanofiber promoting moiety. Gazit's group proposed a strategy of co-assembling several FF containing short peptides into nanotubes, which served as scaffold organizing for Ag and Au NPs. [85].

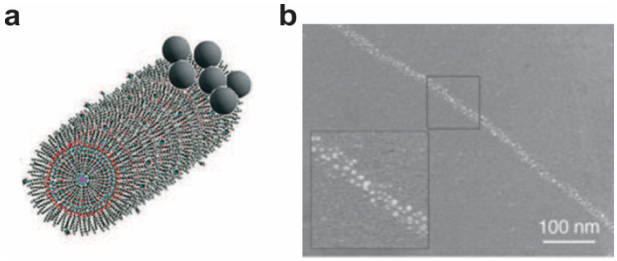

Fig. 1.7. Schematic (a) and TEM images (b) of a tripeptide, fiber-forming amphiphile assisted linear assembly of Au NPs. Reproduced with permission from ref. [37]. Copyright 2005, Wiley-VCH.

In addition to the static assemblies described above, peptides have also been used to prepare dynamic assembly systems. Liedberg *et al.* presented an example of controlling the aggregation state of peptide-capped Au NPs via Zn^{2+} ion-induced peptide folding [86] (Fig. 1.8). Upon addition of Zn^{2+} ions, the polypeptides JR2E, immobilized on the surface of Au NPs, experienced dimerization and folding between two different peptides located on separate particles, thus leading to aggregation of particles. This example provides a new strategy for designing peptide-based Au NP superstructures in a dynamic manner based on responsive behavior of the capping peptides.

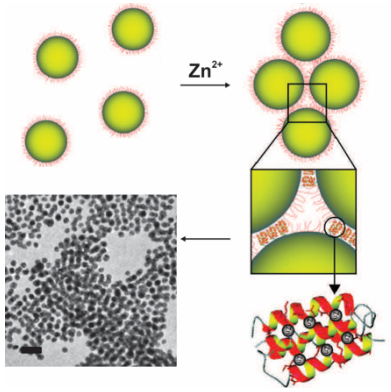

Fig. 1.8. Zn^{2+}-induced aggregation of Au NPs via dimerization of JR2E polypeptides. Scale bar = 50 nm. Reproduced with permission from ref. [86]. Copyright 2008, American Chemical Society.

Ultimately, the goal of assembling NPs is to build new materials that exhibit unique emergent properties based on the organization of the component nanopsrticles. Chiral plasmonic NPs are an interesting subclass of plasmonic nanomaterials, which have many novel optical applications. George *et al.* found that Au nanoparticles grown on FF peptide nanotubes exhibit a bisignated CD signal at their surface plasmon frequency [87] (Fig. 1.9). By changing the chirality of constituent FF peptide used, the overall chirality of Au NP superstructure could be tuned accordingly. The authors found that the chiral peptide nanotube affected the nucleation and growth of Au NPs on the surface of the nanotube, and thus the Au NPs were organized in a chiral manner. It was proposed that these Au nanoparticle assemblies may have potential application in optical devices.

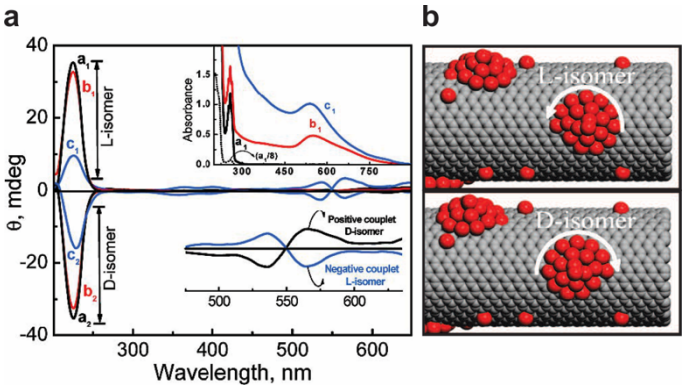

Fig. 1.9. (a) CD signals of Au NP decorated diphenylalanine (FF). (b) Schematic representation of Au NP peptide nanotubes using L- (top) and D-isomers (bottom) of FF peptide nanotube. Reproduced with permission from ref. [87]. Copyright 2010, American Chemical Society.

Other than the common linear fibrils, peptides can also direct the assembly of 2-D arrays of Au NPs. Nonoyama and coworkers designed ordered patterns of Au NPs on a β-sheet peptide template [41] (Fig. 1.10). Adenine-functionalized Au NPs were anchored onto the peptide template via hydrogen bonding with complementary thymine components in the peptide template. Patterning of the Au NPs was easily prepared through the variation of the amino acid sequence to afford a unique 2-D array of Au NPs.

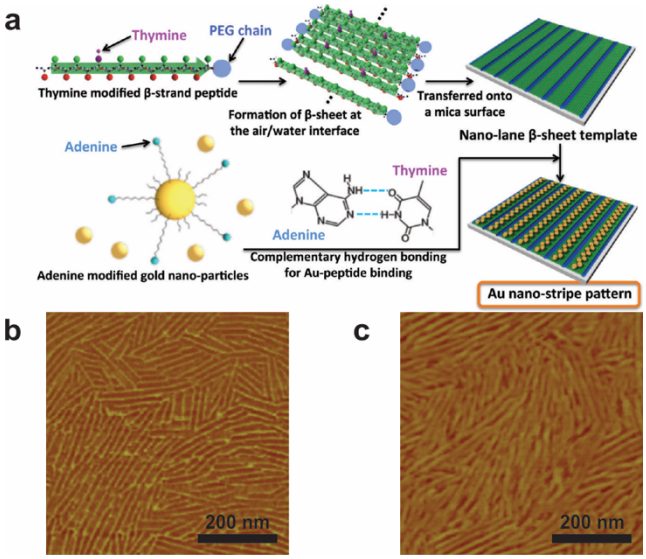

Fig. 1.10. (a) Schematic representation of fabricating 2-D assembly of Au NPs on a β-sheet peptide template. (b, c) Atomic force microscopy (AFM) images of Au NPs assembled on peptide with (b) and without (c) thyminyl groups. Reproduced with permission from ref. [41]. Copyright 2011, American Chemical Society.

Ag NPs, like Au NPs, also exhibit distinct plasmonic resonance properties. Song and coworkers demonstrated that a glutathione-based oligopeptide, Fmoc-GCE, could assemble into nanofibers and promote the incorporation of Ag NPs [88] (Fig. 1.11). Peptide fibrilization was initiated by coordination of Ag^+ ions and the π-π stacking of fluorenyl groups. After adding a proper concentration of reducing agent $NaBH_4$, a linear assembly of Ag NPs were synthesized along the nanofibers. The assembled nanofibers showed high mechanical strength when an appropriate pH of the incubating solvent was reached.

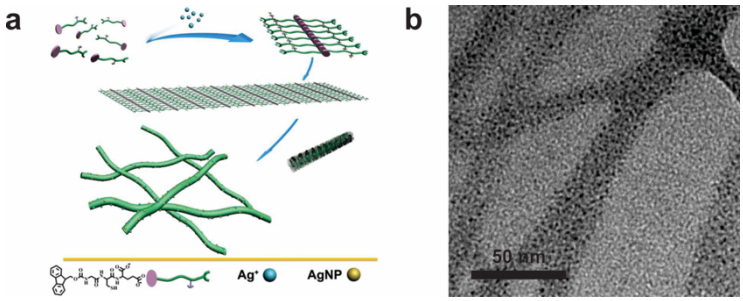

Fig. 1.11. (a) Proposed mechanism for using Fmoc-GCE peptides for assembling Ag NPs. (b) TEM image of assembled Ag NPs assembled along the nanofibers formed by Fmoc-GCE peptides. Reproduced with permission from ref. [88]. Copyright 2015, American Chemical Society.

As peptide-based NP assembly methods continue to evolve, researchers are using them to develop increasingly sophisticated materials. Li and coworkers designed an elegant peptide-mediated Au NP "logic gate", in which the aggregation state of Au NPs could be controlled by the presence of certain enzymes and metal ions [89] (Fig. 1.12). Two functional peptide motifs, i.e. the Zn^{2+} chelating peptide and the protease substrate peptide (chymotrypsin or Chy), were employed as responsive units to Zn^{2+} and enzyme input, respectively. They then capped AuNPs with a carefully designed peptide sequence having a specific response to Zn^{2+} or enzyme. Both the stimuli could affect the aggregation state of Au NPs, leading to the color change of the Au NP colloidal solution. Representative basic binary logic gates such as AND, OR, IMPLICATION, and INHIBIT were developed via this peptide-mediated Au NP assembly system.

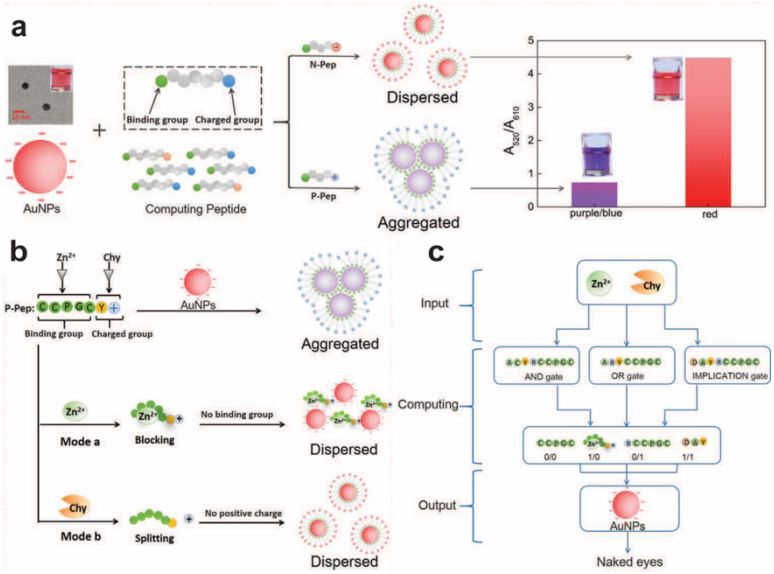

Fig. 1.12. (a) Mechanism of peptide logic gate: the resulting aggregated or dispersed Au NPs shows different colors upon using different combinations of peptides. (b) Aggregation states of Au NPs are controlled by different responses to Zn^{2+} and Chy. (c) The constitution of four logic gates dictated by peptides. Reproduced with permission from ref. [89]. Copyright 2016, American Chemical Society.

More recently, Rodriguez, Rice and coworkers demonstrated Ag NP decorated peptide nanotubes could induce surface-enhanced Raman spectroscopy (SERS) upon UV irradiation [45] (Fig. 1.13). The authors employed the FF peptide nanotube as a scaffold for immobilizing Ag NPs, which were previously proved to support SERS active substrates. When UV irradiation was applied on the Ag NPs aligned on the semiconducting peptide nanotube, SERS from the Ag NPs was significantly enhanced up to 10-fold. This method allowed the detection of many small molecules at concentrations as low as 10^{-13} M. Furthermore, the Ag NP-peptide nanotube prevented photodegradation of the analyte small molecules as the Ag NP superstructure acted as a heat sink upon UV irradiation.

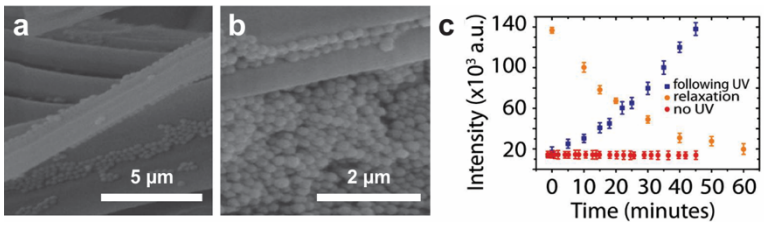

Fig. 1.13. (a, b) SEM images of Ag NPs assembled via diphenylalanine (FF) based peptide nanotubes at two magnifications. (c) Intensity of SERS signal as a function of time following UV irradiation, relaxation after UV irradiation, and in the absence of UV irradiation. Reproduced with permission from ref. [45]. Copyright 2018, Nature Publishing Group.

Peptide-based methods of assembling nanoparticles have also been used for electronic applications. Kang and coworkers used a peptide to mediate programmed deposition of AuPt alloyed NPs on carbon nanotubes (CNTs) that exhibit distinct electrocatalytic activity [90] (Fig. 1.14). A 30-mer peptide, termed HexCoil-Ala, which was designed in a previous study for specific recognition for Au NPs, was used for coating the surfaces of chiral single-walled carbon nanotubes (SWNTs). The positions of the NP binding sites were carefully programmed, which allowed for the helical arrangements of the AuPt NPs. The assembled helical AuPt NPs showed potential in electrocatalytic applications, such as oxygen reduction reactions.

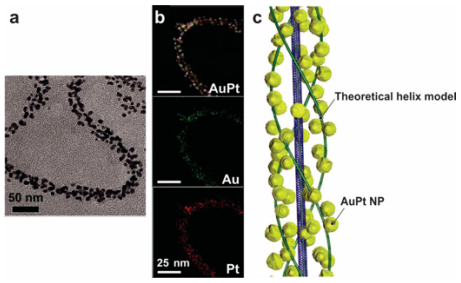

Fig. 1.14. Characterization of AuPt NPs coating the SWNT using the HexCoil-Ala peptides. (a) TEM image. (b) STEM-EDS elemental mapping. (c) 3-D reconstruction of rendered tomographic volume through electron tomography. Reproduced with permission from ref. [90]. Copyright 2018, American Chemical Society.

1.3.2 *One-Pot Synthesis of NP Superstructures*

In the previous section, we discussed how plasmonic NP superstructures were designed and constructed via step-wise syntheses, and we highlighted some of their potential applications. The assembly strategy usually involves 1) peptide template construction, 2) NP synthesis and purification, and 3) NP superstructure formation on the peptide template. It should also be noted that sometimes steps 1) and 2) may occur in a single step where peptide template formation is mediated by a metal precursor. However, combining all of the synthetic steps in a single one-pot procedure may be simpler in practice and reduces the complexity of sample preparation.

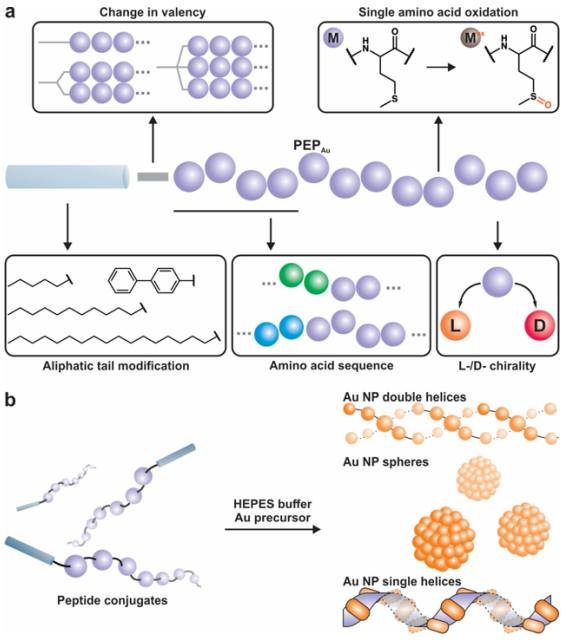

Fig. 1.15. Schematic representation of examples of modification of peptide conjugates and some resulting Au NP superstructures directed by peptide conjugates. (a) Many aspects of peptide conjugates can be systematically modified such as aliphatic tails, valencies, amino acid sequences and chirality, and oxidation state of single amino acid residue. (b) When a certain type of peptide conjugate is dissolved in HEPES buffer in the presence of an Au precursor, various Au NP superstructures are obtained depending on the chosen peptide conjugate.

Rosi and coworkers developed a one-pot peptide-based strategy for synthesizing and assembling NP into structurally well-defined NP superstructures (Fig. 1.15). They have used this strategy to prepare diverse classes of Au NP superstructures, including hollow spheres, double helices, and single helices. These materials were constructed using peptide conjugate molecules that incorporate the Au binding peptide [59, 60], AYSSGAPPMPPF (termed A3 or PEP_{Au}, identified and isolated via phage display method). The peptide conjugates are designed in such a way that they will assemble into a target assembly, such as a 1-D fiber or a spherical vesicle. In a typical NP superstructure synthesis, a specific Au-binding peptide conjugate molecule (R-PEP_{Au}) is dissolved in a mild reducing buffer 4-(2-hydroxyethyl)-1-piperazineethanesulfonic acid (HEPES). Then an aliquot of dissolved Au salt is added. During the synthesis, the Au salt is reduced by the HEPES buffer, forming Au NP. Simultaneously, the Au-binding peptide conjugates bind to the Au particles *and* direct their assembly into a superstructure. The morphology of the NP superstructure is dictated by the assembly of R-PEP_{Au}. In essence, all of the structural features of the product NP superstructure can be programmed into R-PEP_{Au} at the design stage. R-PEP_{Au} is highly tailorable. The 'R' group can be any organic molecule (e.g. aliphatic, aromatic, etc.) and can be designed to be responsive to external stimuli. The PEP_{Au} sequence can also be modified. Rosi and coworkers realized that the N-terminal amino acids of PEP_{Au} (AYSSGA) engage in β-sheet formation, which facilitates the assembly of some R-PEP_{Au} into twisted amyloid-like fibers. This β-sheet region can be modified to adjust the assembly propensity by adding additional hydrophobic amino acids, for example. Finally, the chirality of the amino acids themselves can be either R or S, which can impact the chirality of the resulting assembly. Below, we highlight some of the unique materials prepared using this methodology.

As a first demonstration of the utility of this synthetic method, C_{12}-PEP_{Au} (a 12-carbon aliphatic chain conjugated to PEP_{Au}) was used to direct the synthesis and assembly of AuNP double helices [91] (Fig. 1.16 a-c). It should be highlighted that the assembled Au NP double helices exhibited exceptional structural fidelity; that is, the Au NPs were fairly mono-dispersed (~8 nm), the helical pitch was consistent (~83 nm), and the

predominant product in the synthesis was Au NP double helices. Many structural features, such as NP size and interparticle distances, could be further tuned by adjusting synthetic conditions [92] (Fig. 1.16 d-f). A molecular model for the peptide conjugates was proposed which was then used for the design and rational construction of future superstructures.

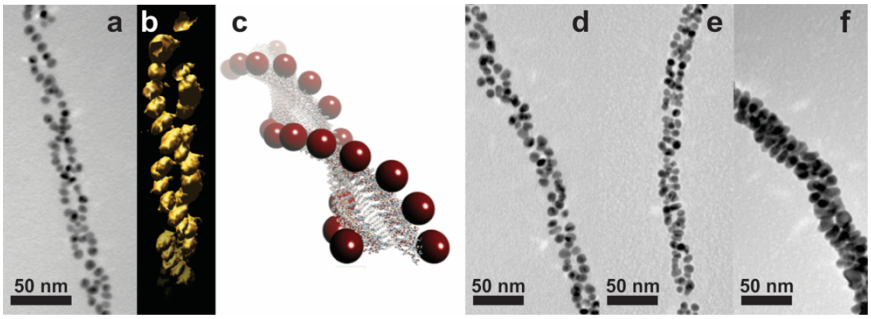

Fig. 1.16. Double helical Au NP superstructures. TEM image (a), rendered tomographic reconstruction image (b), and schematic model (c) of Au NP double helical superstructures directed by peptide conjugate C_{12}-PEP_{Au}. Structural parameters such as constituent NP dimensions (d-f) could be tuned for Au NP double helices. (a-c) Reproduced with permission from ref. [91]. Copyright 2008, American Chemical Society. (d-f) Reproduced with permission from ref. [92]. Copyright 2010, American Chemical Society.

Due to the helical nature of the superstructure, the Au NP double helices exhibited circular dichroism (CD) at the plasmon frequency. As a result, it could be rationally proposed that the handedness of the superstructures could be tuned by using left- or right-handed constituent amino acids. It was then demonstrated that conjugates consisting of all L-amino acid residues yielded left-handed helices and D-amino acid right-handed [93], and mirrored CD signals were observed for these two assemblies, respectively (Fig. 1.17). The experimental CD signals also corresponded well with computational results. These findings demonstrated that rational molecular level modification of the peptide conjugate could be used to control the assembly and chiroptical properties of the helical superstructure.

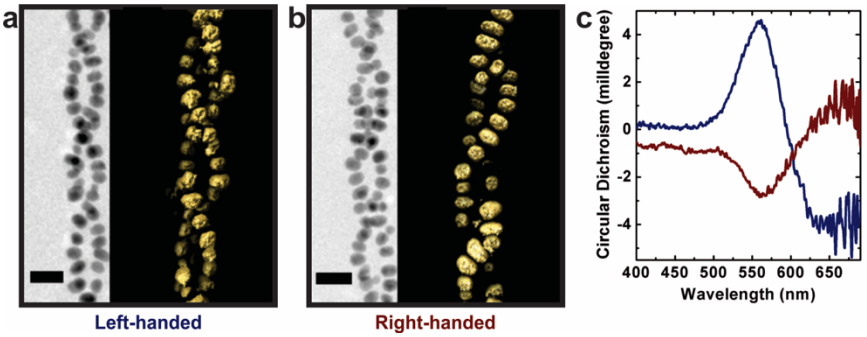

Fig. 1.17. Chirality of the Au NP double helices could be dictated by using all L- or D-amino acids for C_{12}-PEP_{Au} conjugates. (a) Left- and (b) right-handed Au NP double helices are observed under TEM. Scale bar = 20 nm. (c) Mirrored chiroptical signals are observed for the two superstructures respectively. Reproduced with permission from ref [93]. Copyright 2013, American Chemical Society.

A variety of other superstructures were also prepared by systematically modifying the composition of the peptide conjugate. These modifications focus on the following aspects of the conjugates: 1) R-group, 2) the valency of the conjugate (number of the peptides attached to one R-group), and 3) amino acid residues. For example, as an early attempt to explore this strategy, biphenyl groups were conjugated to PEP_{Au} instead of the C_{12} aliphatic chain [94]. It was reasoned that peptide assembly could be promoted due to the π-π stacking interactions of the biphenyl groups. The biphenyl-PEP_{Au} promoted formation of 1-D AuNP assemblies along the peptide fibers.

Based on known design principles for amphiphile assembly, it was known that the length of the aliphatic component could potentially affect the assembly morphology of a peptide conjugate [95]. Thus, tuning the length of the aliphatic chain could lead to variation in the morphology of Au NP superstructures. Following this strategy, spherical Au NP superstructures were prepared by using the peptide conjugate, C_6-AA-PEP_{Au} (a 6-carbon chain conjugated to PEP_{Au} spaced by two additional alanine residues) [96] (Fig. 1.18 a-c). A shorter aliphatic chain allowed for the formation of peptide vesicles instead of peptide fibers. Furthermore, the size of the spherical Au NP superstructure could be tuned by carefully adjusting the synthetic conditions [97]. The resulting Au NP spheres

exhibit a hollow interior. Taking advantage of this feature, it was further shown that these spherical superstructures had potential application in drug-loading and release [98] (Fig. 1.18 d). More specifically, it was demonstrated that the Au NP spheres could take up a common drug doxorubicin (DOX), and upon addition of proteinase K, a non-specific peptidase, large Au NP superstructures (~150 nm in diameter) started to release DOX upon digestion of the peptide scaffold. Additionally, in the presence of light irradiation at 805 nm, both large and medium (~70 nm in diameter) Au NP spheres showed degradation behavior which led to the release of DOX.

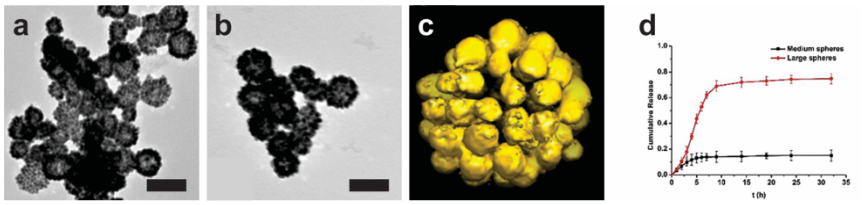

Fig. 1.18. Spherical Au NP superstructures constructed using C_6-AA-PEP_{Au}. (a, b) TEM images of Au NP spherical superstructures. (c) 3-D surface rendering of the tomographic volume of Au NP spheres Reproduced with permission from ref [96]. Copyright 2010, American Chemical Society. (d) Cumulative release profile of DOX-loaded Au NP spheres upon irradiation with 805 nm light. Reproduced with permission from ref [98]. Copyright 2015, Royal Society of Chemistry.

In 2016, a new class of single-helical superstructure with tunable features was constructed using C_x-$(PEP_{Au}{}^{M\text{-}ox})_2$ (x = 16-22, M-ox indicates methionine sulfoxide), in which two PEP_{Au} sequences were tethered to the same aliphatic tail [99-101] (Fig. 1.19 a-f). This family of peptide conjugates assemble into helical ribbons and the Au NPs decorating the helical ribbons were consequently assembled in a single-helical fashion. As the tail length increases from C_{16} to C_{22}, the pitch length of the Au NP helices increases from ~80 nm to ~128 nm, while the size of the constituent Au NPs decreases from ~14 nm to ~6 nm. Meanwhile, the intensity of the corresponding chiroptical signals of the Au NP single helices, which was predicted to be inversely proportional to pitch length, decrease as the aliphatic tail length increases from C_{16} to C_{22}. The CD response of the single helices formed using C_{16}-$(PEP_{Au}{}^{M\text{-}ox})_2$ and C_{18}-$(PEP_{Au}{}^{M\text{-}ox})_2$, as

quantified by the *g*-factor (anisotropic factor), were the highest not only among this family but also among the highest reported for helical NP assemblies (~0.02-0.04). This example demonstrated that simple chemical modifications could be employed to control the helical pitch, the nanoparticle size, and the chiroptical properties within a family of helical nanoparticle superstructures.

Some features of the assembled structures, such as metrics and morphology, could be further adjusted by introducing external reagents. Citrate, another particle capping agent, could be used to affect the dimensions of the NP within the superstructures. [92, 93]. Likewise, it was recently demonstrated that adding an external surfactant, cetyltrimethylammonium bromide (CTAB), could promote anisotropy in the Au NPs within the single-helical superstructures [102], where hexagonal and prismatic particles were observed within the superstructure (Fig. 1.19 g).

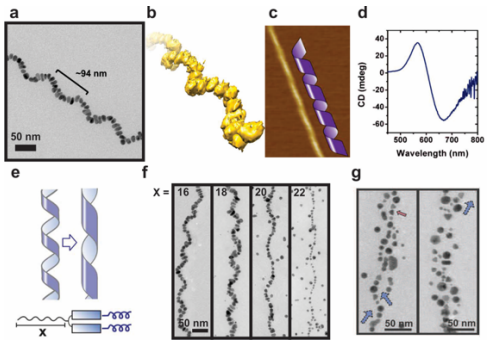

Fig. 1.19. Single helical Au NP superstructures. (a) TEM image and (b) 3-D rendering of tomographic rendering of single helical Au NP superstructures directed by peptide conjugate C_{18}-$(PEP_{Au}{}^{M\text{-}ox})_2$. (c) AFM mapping and schematics representation of the underlying coiled ribbon assembly of peptide conjugate. (d) The resulting Au NP single helices showed enhanced chiroptical response with a *g*-factor of 0.02. Reproduced with permission from ref. [100]. Copyright 2016, American Chemical Society. (e) Schematic illustration of tuning structural features of single helix assembly by modifying the aliphatic tail of peptide conjugate C_x-$(PEP_{Au}{}^{M\text{-}ox})_2$ (x = 16-22). (f) TEM images of single helical Au NP assembly directed by conjugates C_x-$(PEP_{Au}{}^{M\text{-}ox})_2$ (x = 16-22). Reproduced with permission from ref. [100]. Copyright 2017, American Chemical Society. (g) Adding auxiliary particle capping agents to the synthesis of Au NP single helices introduced anisotropy to constituent particles. Reproduced with permission from ref. [102]. Copyright 2018, Wiley-VCH.

As detailed above, this one-pot, single-step methodology presents an easy, simple, and highly tunable approach toward building well-defined Au NP superstructures. Programmable control over the molecular structure of the peptide conjugates allows one to design a diverse collection of superstructures and fine tune their morphology, structural parameters, and physical properties.

1.4 Conclusions and Outlook

The representative examples described in this chapter showcase the versatile role that peptides play in the synthesis and assembly of plasmonic NP. Many challenges and opportunities remain in this exciting field. For example, it remains difficult to predict the assembly and binding capability of a specific peptide based on a given sequence. In contrast, DNA origami can be engineered to access a desired geometry based solely on the design of the base-pair sequence [103]. Many peptide sequences, as mentioned above, are selected via the phage-display method, where a given inorganic surface is provided as a target. Even though this method can isolate peptides that bind to different facets of a NP of the same composition [75], we are still building NP superstructures based on known sequences of peptides. In many cases, the known inorganic-binding peptides may not assemble into target structures. Therefore, it would be ideal if one could rationally modify the peptide sequence to promote its assembly without detrimentally affecting its inorganic recognition capability. Computational studies that examine the role played by individual amino acids for NP binding are helping us understand the assembly and recognition behavior of peptides [104], and may ultimately allow us to rationally design peptides that both bind NP and direct their assembly.

Opportunities also exist in the preparation of dynamic assemblies that respond to external stimuli such as light, pH, ionic strength, pressure, etc. Given the molecular tunability of peptide sequences and peptide conjugates, responsive behavior can potentially be built into the NP superstructures at the molecular level. For example, peptide sequences could be design to bind specific target molecules. Upon binding, the

morphology of the peptide assembly may change, which would lead to a structural change in the NP superstructure and an accompanying perturbation to its plasmonic signal. In this way, sensors for specific molecules could be designed.

1.5 References and Citations

1. Heiligtag, F. J. and Niederberger, M. (2013). The Fascinating World of Nanoparticle Research, Mater. Today, 16, pp. 262-271.
2. Moshfegh, A. Z. (2009). Nanoparticle Catalysts, J. Phys. D: Appl. Phys., 42, pp. 233001.
3. Li, Y., Qian, F., Xiang, J. and Lieber, C. M. (2006). Nanowire Electronic and Optoelectronic Devices, Mater. Today, 9, pp. 18-27.
4. Medintz, I. L., Uyeda, H. T., Goldman, E. R. and Mattoussi, H. (2005). Quantum Dot Bioconjugates for Imaging, Labelling and Sensing, Nat. Mater., 4, pp. 435-446.
5. Stewart, M. E., Anderton, C. R., Thompson, L. B., Maria, J., Gray, S. K., Rogers, J. A. and Nuzzo, R. G. (2008). Nanostructured Plasmonic Sensors, Chem. Rev., 108, pp. 494-521.
6. Tong, L., Wei, Q., Wei, A. and Cheng, J.-X. (2009). Gold Nanorods as Contrast Agents for Biological Imaging: Optical Properties, Surface Conjugation and Photothermal Effects†, Photochem. Photobiol., 85, pp. 21-32.
7. Boles, M. A., Engel, M. and Talapin, D. V. (2016). Self-Assembly of Colloidal Nanocrystals: From Intricate Structures to Functional Materials, Chem. Rev., 116, pp. 11220-11289.
8. Maier, S. A. and Atwater, H. A. (2005). Plasmonics: Localization and Guiding of Electromagnetic Energy in Metal/Dielectric Structures, J. Appl. Phys., 98, pp. 011101.
9. Ozbay, E. (2006). Plasmonics: Merging Photonics and Electronics at Nanoscale Dimensions, Science, 311, pp. 189-193.
10. Tang, Z., Wang, Y., Podsiadlo, P. and Kotov, N. A. (2006). Biomedical Applications of Layer-by-Layer Assembly: From Biomimetics to Tissue Engineering, Adv. Mater., 18, pp. 3203-3224.
11. Zeng, S., Baillargeat, D., Ho, H.-P. and Yong, K.-T. (2014). Nanomaterials Enhanced Surface Plasmon Resonance for Biological and Chemical Sensing Applications, Chem. Soc. Rev., 43, pp. 3426-3452.
12. Whaley, S. R., English, D. S., Hu, E. L., Barbara, P. F. and Belcher, A. M. (2000). Selection of Peptides with Semiconductor Binding Specificity for Directed Nanocrystal Assembly, Nature, 405, pp. 665-668.

13. Lee, K.-S. and El-Sayed, M. A. (2006). Gold and Silver Nanoparticles in Sensing and Imaging: Sensitivity of Plasmon Response to Size, Shape, and Metal Composition, J. Phys. Chem. B, 110, pp. 19220-19225.
14. Anker, J. N., Hall, W. P., Lyandres, O., Shah, N. C., Zhao, J. and Van Duyne, R. P. (2008). Biosensing with Plasmonic Nanosensors, Nat. Mater., 7, pp. 442-453.
15. Couvreur, P. (2013). Nanoparticles in Drug Delivery: Past, Present and Future, Adv. Drug Deliv. Rev., 65, pp. 21-23.
16. Agasti, S. S., Chompoosor, A., You, C.-C., Ghosh, P., Kim, C. K. and Rotello, V. M. (2009). Photoregulated Release of Caged Anticancer Drugs from Gold Nanoparticles, J. Am. Chem. Soc., 131, pp. 5728-5729.
17. Cheng, Y., Samia, A. C., Li, J., Kenney, M. E., Resnick, A. and Burda, C. (2010). Delivery and Efficacy of a Cancer Drug as a Function of the Bond to the Gold Nanoparticle Surface, Langmuir, 26, pp. 2248-2255.
18. Doane, T. L. and Burda, C. (2012). The Unique Role of Nanoparticles in Nanomedicine: Imaging, Drug Delivery and Therapy, Chem. Soc. Rev., 41, pp. 2885-2911.
19. Nam, J., La, W.-G., Hwang, S., Ha, Y. S., Park, N., Won, N., Jung, S., Bhang, S. H., Ma, Y.-J., Cho, Y.-M., Jin, M., Han, J., Shin, J.-Y., Wang, E. K., Kim, S. G., Cho, S.-H., Yoo, J., Kim, B.-S. and Kim, S. (2013). Ph-Responsive Assembly of Gold Nanoparticles and "Spatiotemporally Concerted" Drug Release for Synergistic Cancer Therapy, ACS Nano, 7, pp. 3388-3402.
20. Tadepalli, S., Kuang, Z., Jiang, Q., Liu, K.-K., Fisher, M. A., Morrissey, J. J., Kharasch, E. D., Slocik, J. M., Naik, R. R. and Singamaneni, S. (2015). Peptide Functionalized Gold Nanorods for the Sensitive Detection of a Cardiac Biomarker Using Plasmonic Paper Devices, Sci. Rep., 5, pp. 16206.
21. Tang, L., Li, S., Xu, L., Ma, W., Kuang, H., Wang, L. and Xu, C. (2015). Chirality-Based Au@Ag Nanorod Dimers Sensor for Ultrasensitive Psa Detection, ACS Appl. Mater. Interfaces, 7, pp. 12708-12712.
22. Willets, K. A. and Van Duyne, R. P. (2007). Localized Surface Plasmon Resonance Spectroscopy and Sensing, Annu. Rev. Phys. Chem., 58, pp. 267-297.
23. Kamat, P. V. (2002). Photophysical, Photochemical and Photocatalytic Aspects of Metal Nanoparticles, J. Phys. Chem. B, 106, pp. 7729-7744.
24. Daniel, M. C. and Astruc, D. (2004). Gold Nanoparticles: Assembly, Supramolecular Chemistry, Quantum-Size-Related Properties, and Applications toward Biology, Catalysis, and Nanotechnology, Chem. Rev., 104, pp. 293-346.
25. Mostafa, S., Behafarid, F., Croy, J. R., Ono, L. K., Li, L., Yang, J. C., Frenkel, A. I. and Cuenya, B. R. (2010). Shape-Dependent Catalytic Properties of Pt Nanoparticles, J. Am. Chem. Soc., 132, pp. 15714-15719.
26. Wei, Y., Han, S., Kim, J., Soh, S. and Grzybowski, B. A. (2010). Photoswitchable Catalysis Mediated by Dynamic Aggregation of Nanoparticles, J. Am. Chem. Soc., 132, pp. 11018-11020.

27. Maier, S. A. (2007) *Plasmonics: Fundamentals and Applications*, (Springer US, New York, NY).
28. Kelly, K. L., Coronado, E., Zhao, L. L. and Schatz, G. C. (2003). The Optical Properties of Metal Nanoparticles: The Influence of Size, Shape, and Dielectric Environment, J. Phys. Chem. B, 107, pp. 668-677.
29. Lee, K.-S. and El-Sayed, M. A. (2006). Gold and Silver Nanoparticles in Sensing and Imaging: Sensitivity of Plasmon Response to Size, Shape, and Metal Composition, J. Phys. Chem. B, 110, pp. 19220-19225.
30. Skrabalak, S. E., Au, L., Li, X. and Xia, Y. (2007). Facile Synthesis of Ag Nanocubes and Au Nanocages, Nat. Protoc., 2, pp. 2182-2190.
31. Gurunatha, K. L., Fournier, A. C., Urvoas, A., Valerio-Lepiniec, M., Marchi, V., Minard, P. and Dujardin, E. (2016). Nanoparticles Self-Assembly Driven by High Affinity Repeat Protein Pairing, ACS Nano, 10, pp. 3176-3185.
32. Cai, C., Lin, J., Lu, Y., Zhang, Q. and Wang, L. (2016). Polypeptide Self-Assemblies: Nanostructures and Bioapplications, Chem. Soc. Rev., 45, pp. 5985-6012.
33. Adler-Abramovich, L. and Gazit, E. (2014). The Physical Properties of Supramolecular Peptide Assemblies: From Building Block Association to Technological Applications, Chem. Soc. Rev., 43, pp. 6881-6893.
34. Kim, S., Kim, J. H., Lee, J. S. and Park, C. B. (2015). Beta-Sheet-Forming, Self-Assembled Peptide Nanomaterials Towards Optical, Energy, and Healthcare Applications, Small, 11, pp. 3623-3640.
35. Kumar, J., Eraña, H., López-Martínez, E., Claes, N., Martín, V. F., Solís, D. M., Bals, S., Cortajarena, A. L., Castilla, J. and Liz-Marzán, L. M. (2018). Detection of Amyloid Fibrils in Parkinson's Disease Using Plasmonic Chirality, Proc. Natl. Acad. Sci. U. S. A., 115, pp. 3225.
36. Reches, M. and Gazit, E. (2004). Formation of Closed-Cage Nanostructures by Self-Assembly of Aromatic Dipeptides, Nano Lett., 4, pp. 581-585.
37. Li, L.-s. and Stupp, S. I. (2005). One-Dimensional Assembly of Lipophilic Inorganic Nanoparticles Templated by Peptide-Based Nanofibers with Binding Functionalities, Angew. Chem. Int. Ed., 44, pp. 1833-1836.
38. Hendricks, M. P., Sato, K., Palmer, L. C. and Stupp, S. I. (2017). Supramolecular Assembly of Peptide Amphiphiles, Acc. Chem. Res., 50, pp. 2440-2448.
39. Wei, G., Su, Z., Reynolds, N. P., Arosio, P., Hamley, I. W., Gazit, E. and Mezzenga, R. (2017). Self-Assembling Peptide and Protein Amyloids: From Structure to Tailored Function in Nanotechnology, Chem. Soc. Rev., 46, pp. 4661-4708.
40. Hamley, I. W., Dehsorkhi, A. and Castelletto, V. (2013). Self-Assembled Arginine-Coated Peptide Nanosheets in Water, Chem. Commun., 49, pp. 1850-1852.
41. Nonoyama, T., Tanaka, M., Inai, Y., Higuchi, M. and Kinoshita, T. (2011). Ordered Nanopattern Arrangement of Gold Nanoparticles on B-Sheet Peptide Templates through Nucleobase Pairing, ACS Nano, 5, pp. 6174-6183.
42. Hamley, I. W. and Castelletto, V. (2017). Self-Assembly of Peptide Bioconjugates: Selected Recent Research Highlights, Bioconjugate Chem., 28, pp. 731-739.

43. Xie, X., Wang, L., Liu, X., Du, Z., Li, Y., Li, B., Wu, L. and Li, W. (2020). Light-Powered and Transient Peptide Two-Dimensional Assembly Driven by Trans-to-Cis Isomerization of Azobenzene Side Chains, Chem. Commun., 10.1039/C9CC09448B, pp.
44. Taskova, M., Madsen, C. S., Jensen, K. J., Hansen, L. H., Vester, B. and Astakhova, K. (2017). Antisense Oligonucleotides Internally Labeled with Peptides Show Improved Target Recognition and Stability to Enzymatic Degradation, Bioconjugate Chem., 28, pp. 768-774.
45. Almohammed, S., Zhang, F., Rodriguez, B. J. and Rice, J. H. (2018). Photo-Induced Surface-Enhanced Raman Spectroscopy from a Diphenylalanine Peptide Nanotube-Metal Nanoparticle Template, Sci. Rep., 8, pp. 3880.
46. Gao, X. and Matsui, H. (2005). Peptide-Based Nanotubes and Their Applications in Bionanotechnology, Adv. Mater., 17, pp. 2037-2050.
47. de la Rica, R. and Matsui, H. (2010). Applications of Peptide and Protein-Based Materials in Bionanotechnology, Chem. Soc. Rev., 39, pp. 3499-3509.
48. Zong, J., Cobb, S. L. and Cameron, N. R. (2017). Peptide-Functionalized Gold Nanoparticles: Versatile Biomaterials for Diagnostic and Therapeutic Applications, Biomater. Sci., 5, pp. 872-886.
49. Tiede, C., Tang, A. A. S., Deacon, S. E., Mandal, U., Nettleship, J. E., Owen, R. L., George, S. E., Harrison, D. J., Owens, R. J., Tomlinson, D. C. and McPherson, M. J. (2014). Adhiron: A Stable and Versatile Peptide Display Scaffold for Molecular Recognition Applications, Protein Eng. Des. Sel., 27, pp. 145-155.
50. Hoshino, Y., Koide, H., Urakami, T., Kanazawa, H., Kodama, T., Oku, N. and Shea, K. J. (2010). Recognition, Neutralization, and Clearance of Target Peptides in the Bloodstream of Living Mice by Molecularly Imprinted Polymer Nanoparticles: A Plastic Antibody, J. Am. Chem. Soc., 132, pp. 6644-6645.
51. Chen, C.-L. and Rosi, N. L. (2010). Peptide-Based Methods for the Preparation of Nanostructured Inorganic Materials, Angew. Chem. Int. Ed., 49, pp. 1924-1942.
52. Pierschbacher, M. D. and Ruoslahti, E. (1984). Cell Attachment Activity of Fibronectin Can Be Duplicated by Small Synthetic Fragments of the Molecule, Nature, 309, pp. 30-33.
53. Webber, M. J., Tongers, J., Renault, M.-A., Roncalli, J. G., Losordo, D. W. and Stupp, S. I. (2010). Development of Bioactive Peptide Amphiphiles for Therapeutic Cell Delivery, Acta Biomater., 6, pp. 3-11.
54. Birnbaum, Michael E., Mendoza, Juan L., Sethi, Dhruv K., Dong, S., Glanville, J., Dobbins, J., Özkan, E., Davis, Mark M., Wucherpfennig, Kai W. and Garcia, K. C. (2014). Deconstructing the Peptide-Mhc Specificity of T Cell Recognition, Cell, 157, pp. 1073-1087.
55. Hersel, U., Dahmen, C. and Kessler, H. (2003). Rgd Modified Polymers: Biomaterials for Stimulated Cell Adhesion and Beyond, Biomaterials, 24, pp. 4385-4415.

56. Danhier, F., Le Breton, A. and Préat, V. (2012). Rgd-Based Strategies to Target Alpha(V) Beta(3) Integrin in Cancer Therapy and Diagnosis, Molecular Pharmaceutics, 9, pp. 2961-2973.
57. Dickerson, M. B., Sandhage, K. H. and Naik, R. R. (2008). Protein- and Peptide-Directed Syntheses of Inorganic Materials, Chem. Rev., 108, pp. 4935-4978.
58. Yang, W., Guo, W., Chang, J. and Zhang, B. (2017). Protein/Peptide-Templated Biomimetic Synthesis of Inorganic Nanoparticles for Biomedical Applications, J. Mater. Chem. B, 5, pp. 401-417.
59. Naik, R. R., Stringer, S. J., Agarwal, G., Jones, S. E. and Stone, M. O. (2002). Biomimetic Synthesis and Patterning of Silver Nanoparticles, Nat. Mater., 1, pp. 169-172.
60. Slocik, J. M., Stone, M. O. and Naik, R. R. (2005). Synthesis of Gold Nanoparticles Using Multifunctional Peptides, Small, 1, pp. 1048-1052.
61. Djalali, R., Chen, Y.-f. and Matsui, H. (2002). Au Nanowire Fabrication from Sequenced Histidine-Rich Peptide, J. Am. Chem. Soc., 124, pp. 13660-13661.
62. Slocik, J. M., Moore, J. T. and Wright, D. W. (2002). Monoclonal Antibody Recognition of Histidine-Rich Peptide Encapsulated Nanoclusters, Nano Lett., 2, pp. 169-173.
63. Hnilova, M., Oren, E. E., Seker, U. O. S., Wilson, B. R., Collino, S., Evans, J. S., Tamerler, C. and Sarikaya, M. (2008). Effect of Molecular Conformations on the Adsorption Behavior of Gold-Binding Peptides, Langmuir, 24, pp. 12440-12445.
64. Brown, S. (1997). Metal-Recognition by Repeating Polypeptides, Nat. Biotechnol., 15, pp. 269-272.
65. Seker, U. O. S., Wilson, B., Kulp, J. L., Evans, J. S., Tamerler, C. and Sarikaya, M. (2014). Thermodynamics of Engineered Gold Binding Peptides: Establishing the Structure–Activity Relationships, Biomacromolecules, 15, pp. 2369-2377.
66. Yu, L., Banerjee, I. A. and Matsui, H. (2003). Direct Growth of Shape-Controlled Nanocrystals on Nanotubes Via Biological Recognition, J. Am. Chem. Soc., 125, pp. 14837-14840.
67. Banerjee, I. A., Yu, L. and Matsui, H. (2003). Cu Nanocrystal Growth on Peptide Nanotubes by Biomineralization: Size Control of Cu Nanocrystals by Tuning Peptide Conformation, Proc. Natl. Acad. Sci. U. S. A., 100, pp. 14678.
68. Slocik, J. M. and Wright, D. W. (2003). Biomimetic Mineralization of Noble Metal Nanoclusters, Biomacromolecules, 4, pp. 1135-1141.
69. Sarikaya, M., Tamerler, C., Jen, A. K. Y., Schulten, K. and Baneyx, F. (2003). Molecular Biomimetics: Nanotechnology through Biology, Nat. Mater., 2, pp. 577-585.
70. Brown, S., Sarikaya, M. and Johnson, E. (2000). A Genetic Analysis of Crystal Growth11edited by M. Gottesman, Journal of Molecular Biology, 299, pp. 725-735.
71. Huang, Y., Chiang, C.-Y., Lee, S. K., Gao, Y., Hu, E. L., Yoreo, J. D. and Belcher, A. M. (2005). Programmable Assembly of Nanoarchitectures Using Genetically Engineered Viruses, Nano Lett., 5, pp. 1429-1434.

72. Nam, K. T., Kim, D.-W., Yoo, P. J., Chiang, C.-Y., Meethong, N., Hammond, P. T., Chiang, Y.-M. and Belcher, A. M. (2006). Virus-Enabled Synthesis and Assembly of Nanowires for Lithium Ion Battery Electrodes, Science, 312, pp. 885.
73. Wei, Z., Maeda, Y. and Matsui, H. (2011). Discovery of Catalytic Peptides for Inorganic Nanocrystal Synthesis by a Combinatorial Phage Display Approach, Angew. Chem. Int. Ed., 50, pp. 10585-10588.
74. Umetsu, M., Mizuta, M., Tsumoto, K., Ohara, S., Takami, S., Watanabe, H., Kumagai, I. and Adschiri, T. (2005). Bioassisted Room-Temperature Immobilization and Mineralization of Zinc Oxide—the Structural Ordering of Zno Nanoparticles into a Flower-Type Morphology, Adv. Mater., 17, pp. 2571-2575.
75. Chiu, C.-Y., Li, Y., Ruan, L., Ye, X., Murray, C. B. and Huang, Y. (2011). Platinum Nanocrystals Selectively Shaped Using Facet-Specific Peptide Sequences, Nat. Chem., 3, pp. 393-399.
76. Peelle, B. R., Krauland, E. M., Wittrup, K. D. and Belcher, A. M. (2005). Probing the Interface between Biomolecules and Inorganic Materials Using Yeast Surface Display and Genetic Engineering, Acta Biomater., 1, pp. 145-154.
77. Flynn, C. E., Mao, C., Hayhurst, A., Williams, J. L., Georgiou, G., Iverson, B. and Belcher, A. M. (2003). Synthesis and Organization of Nanoscale Ii–Vi Semiconductor Materials Using Evolved Peptide Specificity and Viral Capsid Assembly, J. Mater. Chem., 13, pp. 2414-2421.
78. Mao, C., Solis, D. J., Reiss, B. D., Kottmann, S. T., Sweeney, R. Y., Hayhurst, A., Georgiou, G., Iverson, B. and Belcher, A. M. (2004). Virus-Based Toolkit for the Directed Synthesis of Magnetic and Semiconducting Nanowires, Science, 303, pp. 213.
79. Reiss, B. D., Mao, C., Solis, D. J., Ryan, K. S., Thomson, T. and Belcher, A. M. (2004). Biological Routes to Metal Alloy Ferromagnetic Nanostructures, Nano Lett., 4, pp. 1127-1132.
80. Khoo, X., Hamilton, P., O'Toole, G. A., Snyder, B. D., Kenan, D. J. and Grinstaff, M. W. (2009). Directed Assembly of Pegylated-Peptide Coatings for Infection-Resistant Titanium Metal, J. Am. Chem. Soc., 131, pp. 10992-10997.
81. Sano, K.-I., Sasaki, H. and Shiba, K. (2005). Specificity and Biomineralization Activities of Ti-Binding Peptide-1 (Tbp-1), Langmuir, 21, pp. 3090-3095.
82. Fu, X., Wang, Y., Huang, L., Sha, Y., Gui, L., Lai, L. and Tang, Y. (2003). Assemblies of Metal Nanoparticles and Self-Assembled Peptide Fibrils—Formation of Double Helical and Single-Chain Arrays of Metal Nanoparticles, Adv. Mater., 15, pp. 902-906.
83. Wong, M. S., Cha, J. N., Choi, K.-S., Deming, T. J. and Stucky, G. D. (2002). Assembly of Nanoparticles into Hollow Spheres Using Block Copolypeptides, Nano Lett., 2, pp. 583-587.
84. Stevens, M. M., Flynn, N. T., Wang, C., Tirrell, D. A. and Langer, R. (2004). Coiled-Coil Peptide-Based Assembly of Gold Nanoparticles, Adv. Mater., 16, pp. 915-918.

85. Carny, O., Shalev, D. E. and Gazit, E. (2006). Fabrication of Coaxial Metal Nanocables Using a Self-Assembled Peptide Nanotube Scaffold, Nano Lett., 6, pp. 1594-1597.
86. Aili, D., Enander, K., Rydberg, J., Nesterenko, I., Björefors, F., Baltzer, L. and Liedberg, B. (2008). Folding Induced Assembly of Polypeptide Decorated Gold Nanoparticles, J. Am. Chem. Soc., 130, pp. 5780-5788.
87. George, J. and Thomas, K. G. (2010). Surface Plasmon Coupled Circular Dichroism of Au Nanoparticles on Peptide Nanotubes, J. Am. Chem. Soc., 132, pp. 2502-2503.
88. Hu, Y., Xu, W., Li, G., Xu, L., Song, A. and Hao, J. (2015). Self-Assembled Peptide Nanofibers Encapsulated with Superfine Silver Nanoparticles Via Ag+ Coordination, Langmuir, 31, pp. 8599-8605.
89. Li, Y., Li, W., He, K.-Y., Li, P., Huang, Y., Nie, Z. and Yao, S.-Z. (2016). A Biomimetic Colorimetric Logic Gate System Based on Multi-Functional Peptide-Mediated Gold Nanoparticle Assembly, Nanoscale, 8, pp. 8591-8599.
90. Kang, E. S., Kim, Y.-T., Ko, Y.-S., Kim, N. H., Cho, G., Huh, Y. H., Kim, J.-H., Nam, J., Thach, T. T., Youn, D., Kim, Y. D., Yun, W. S., DeGrado, W. F., Kim, S. Y., Hammond, P. T., Lee, J., Kwon, Y.-U., Ha, D.-H. and Kim, Y. H. (2018). Peptide-Programmable Nanoparticle Superstructures with Tailored Electrocatalytic Activity, ACS Nano, 12, pp. 6554-6562.
91. Chen, C.-L., Zhang, P. and Rosi, N. L. (2008). A New Peptide-Based Method for the Design and Synthesis of Nanoparticle Superstructures: Construction of Highly Ordered Gold Nanoparticle Double Helices, J. Am. Chem. Soc., 130, pp. 13555-13557.
92. Chen, C.-L. and Rosi, N. L. (2010). Preparation of Unique 1-D Nanoparticle Superstructures and Tailoring Their Structural Features, J. Am. Chem. Soc., 132, pp. 6902-6903.
93. Song, C., Blaber, M. G., Zhao, G., Zhang, P., Fry, H. C., Schatz, G. C. and Rosi, N. L. (2013). Tailorable Plasmonic Circular Dichroism Properties of Helical Nanoparticle Superstructures, Nano Lett., 13, pp. 3256-3261.
94. Hwang, L., Chen, C.-L. and Rosi, N. L. (2011). Preparation of 1-D Nanoparticle Superstructures with Tailorable Thicknesses Using Gold-Binding Peptide Conjugates, Chem. Commun., 47, pp. 185-187.
95. Shimizu, T., Masuda, M. and Minamikawa, H. (2005). Supramolecular Nanotube Architectures Based on Amphiphilic Molecules, Chem. Rev., 105, pp. 1401-1444.
96. Song, C., Zhao, G., Zhang, P. and Rosi, N. L. (2010). Expeditious Synthesis and Assembly of Sub-100 Nm Hollow Spherical Gold Nanoparticle Superstructures, J. Am. Chem. Soc., 132, pp. 14033-14035.
97. Zhang, C., Zhou, Y., Merg, A., Song, C., Schatz, G. C. and Rosi, N. L. (2014). Hollow Spherical Gold Nanoparticle Superstructures with Tunable Diameters and Visible to near-Infrared Extinction, Nanoscale, 6, pp. 12328-12332.

98. Zhang, C., Brinzer, T., Liu, C., Garrett-Roe, S. and Rosi, N. L. (2015). Loading and Triggered Release of Cargo from Hollow Spherical Gold Nanoparticle Superstructures, Rsc Advances, 5, pp. 76291-76295.
99. Merg, A. D., Slocik, J., Blaber, M. G., Schatz, G. C., Naik, R. and Rosi, N. L. (2015). Adjusting the Metrics of 1-D Helical Gold Nanoparticle Superstructures Using Multivalent Peptide Conjugates, Langmuir, 31, pp. 9492-9501.
100. Merg, A. D., Boatz, J. C., Mandal, A., Zhao, G., Mokashi-Punekar, S., Liu, C., Wang, X., Zhang, P., van der Wel, P. C. A. and Rosi, N. L. (2016). Peptide-Directed Assembly of Single-Helical Gold Nanoparticle Superstructures Exhibiting Intense Chiroptical Activity, J. Am. Chem. Soc., 138, pp. 13655-13663.
101. Mokashi-Punekar, S., Merg, A. D. and Rosi, N. L. (2017). Systematic Adjustment of Pitch and Particle Dimensions within a Family of Chiral Plasmonic Gold Nanoparticle Single Helices, J. Am. Chem. Soc., 139, pp. 15043-15048.
102. Mokashi‐Punekar, S. and Rosi, N. L. (2019). Deliberate Introduction of Particle Anisotropy in Helical Gold Nanoparticle Superstructures, Part. Part. Syst. Char., 36, pp.
103. Rothemund, P. W. K. (2006). Folding DNA to Create Nanoscale Shapes and Patterns, Nature, 440, pp. 297-302.
104. Munro, C. J., Hughes, Z. E., Walsh, T. R. and Knecht, M. R. (2016). Peptide Sequence Effects Control the Single Pot Reduction, Nucleation, and Growth of Au Nanoparticles, J. Phys. Chem. C, 120, pp. 18917-18924.